




# Impact of Solar Radiation on Hygrothermal Behavior of a Washing Fine Hemp Wall

Naima Boumediene<sup>1,2</sup>(✉), Sylvie Prétot<sup>1</sup>, Florence Collet<sup>1</sup> , and Geoffrey Promis<sup>2</sup>

<sup>1</sup> Laboratoire Génie Civil et Génie Mécanique, Université de Rennes, 35704 Rennes, France

<sup>2</sup> Laboratoire de Technologie Innovantes, Université de Picardie Jules Verne, 80025 Amiens, France

naima.boumediene@u-picardie.fr

**Abstract.** The hygrothermal behavior of Washing Fines Hemp Composites was investigated experimentally and numerically at the wall scale for several French and Tunisian climates without considering solar gains nor rain. The stabilization phase leads to experimental and numerical thermal conductive resistance consistent with the theoretical one. The hygric resistance is consistent for simulation performed up to steady state. The profiles at different time during daily climate cycles show that two thirds of the thickness of the wall on the exterior side are active and sorption-desorption phenomena occur in the wall.

This paper investigates the impact of solar radiation on the hygrothermal behavior of a WFH wall under typical French summer climate. The experimental study is performed with a dual-climatic rooms that simulates the indoor and outdoor climates where the solar radiation is taken into account with equivalent outdoor temperature. The test wall is instrumented with temperature and Relative Humidity sensors and with heat flux sensors.

The responses of the wall are analyzed from the temperature and vapor pressure kinetics and profiles. Thermal and hygric penetration depth are similar as the ones obtained without solar gains. Heat storage and sorption-desorption phenomena are enhanced by solar gains.

**Keywords:** Bio-based material · bi-climatic set up · summer climate

## 1 Introduction

Sustainable development is one of the main challenges of recent years. It encourages the use of building materials with low environmental impact and high hygrothermal performance in order to reduce energy consumption. Bio-based materials, made of particles or plant fibres, are one of these materials, which offer competitive thermal and environmental performance (Amziane et al. 2017). In this context, Washing Fines Hemp composites have been developed and characterised at the material scale at LGCGM (Mazhoud et al. 2017). They show good thermal and hygric performances such as low thermal conductivity about  $0.11 \text{ W.m}^{-1}.\text{K}^{-1}$  and high moisture buffer ability with MBV equal to  $2.24 \text{ g.m}^{-2}.\%RH^{-1}$  for a density of  $448 \text{ kg.m}^{-3}$  (Mazhoud et al. 2021). Their

characterisation at the wall scale is a necessary intermediate step before moving onto building-scale construction (Medjelekh et al. 2017; Seng et al. 2021). In a previous step, the hygrothermal behavior of this material was investigated experimentally and numerically at the wall scale for several French and Tunisian climates without considering solar gains nor rain (Boumediene et al. 2022).

Thus, this study focuses on the impact of solar radiation on the hygrothermal characterisation of a Washing Fines Hemp wall under typical French summer climate. The experimental study is performed with a bi-climatic rooms that simulates the indoor and outdoor climates where the solar radiation is taken into account with equivalent outdoor temperature.

The first part of this paper presents the experimental device. Then, the kinetic are presented all along the test. The results are analyzed in the dynamic phase from temperature and vapor pressure kinetics at several depth in the wall and temperature and vapor pressure profiles at several times in both cases with and without solar radiation. Finally, this study underline that heat storage and sorption-desorption phenomena are enhanced by solar gains.

## 2 Methods

### 2.1 Experimental Device and Metrology

The experimental set-up consists in dual-climatic rooms (Fig. 1a): each room is 2.35 m deep, 2.78 m wide and 2.4 m high. The floor is built of concrete; the outside walls and the ceiling are insulated from heat and moisture with air proof polyurethane panels. The two rooms are controlled in temperature and relative humidity to simulate the indoor and the outdoor climates. Their respective temperature and humidity ranges are 18 to 27 °C / -5 to 35 °C and 30 to 60%RH / 30 to 90%RH. Each parameter (T and RH) is regulated by a DR4020 universal controller that acts on convectors for heating, cooling unit for dehumidification and refrigeration and ultrasonic humidifiers for humidification.

These rooms are separated by wall that can be as a whole (Collet and Prétot 2014) or divided into several parts to compare various wall compositions simultaneously. The studied wall is 1.1 cm long and 1 m high. It consists in a 28 cm thick layer of washing fine – hemp composite (WFH), coated with a 0.3 cm thick skincoat clay plaster (SCP) on the indoor side and with 3 cm thick hemp-lime render (HLR) on the outdoor side (Fig. 1b).

The hygrothermal behavior of the wall is supervised with ten SHT35 Sensirion sensors used as ambience sensors and distributed along thickness of the wall (Fig. 1c, d). The accuracy of these sensors is  $\pm 0.1$  °C for a range from 20 °C to 60 °C of temperature and  $\pm 1.5\%$  of relative humidity up to 80%RH at 25 °C. The time step for data acquisition is five minutes. The heat flux is measured on the indoor and on the outdoor surfaces of the wall with HFP01 heat flux sensors from Hukseflux (80 mm in diameter and 5 mm thick). The sensors are oriented so that the heat flux is positive from the indoor side to the outdoor side of the wall.

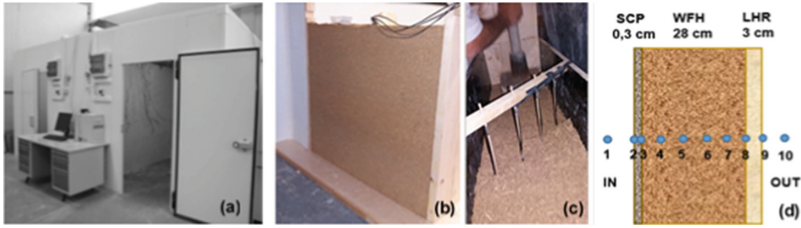


**Fig. 1.** Experimental device (a), WFH wall (b), implementation of hygrothermal sensors (c), sensors positions (d)

**2.2 Solicitations**

This study aims to investigate the effect of solar radiation on the hygrothermal behavior of the WFH wall for a sub-oceanic climate corresponding to the city of Rennes, in France, during the summer. The indoor conditions are constants, with temperature of 23 °C and relative humidity of 50% RH. The outdoor conditions correspond to a typical day that is chosen to be representative of the minimum and maximum 30-year average temperatures in August (1981–2010, Météo France. (2022)). The effect of solar radiation is taken into account with an equivalent temperature calculated from the solar radiation of the cities (Fig. 2). The relative humidity is calculated from vapor pressure and equivalent temperature (Eq. 1).

$$T_{eq} = T_a + \alpha \phi_r R_{se} \tag{1}$$

- $T_{eq}$ : equivalent temperature (°C).
- $T_a$ : outdoor ambient temperature (°C).
- $\alpha$  absorption coefficient .
- $\phi_r$ : solar radiation ( $W/m^2$ ).
- $R_{se}$ : exchange surface resistance ( $m^2.K.W^{-1}$ ).

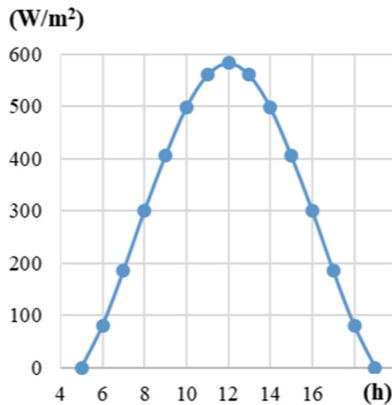


**Fig. 2.** Solar radiation for one typical day in Rennes in August (‘Diagramme Solaire Interactif’ 2022)

Firstly, the wall is stabilized at night conditions until the temperature/vapor pressure variation is lower than 1% / 2% over the last 24 h at each position. This needs up to 15 days. The wall is then exposed to daily cyclic variations. The cycles are performed several times until a repeatable response of the hygrothermal behavior of the wall is obtained. The repeatability is reached when the temperature/vapor pressure variation is lower than 1% / 2% between the last two cycles at each position. This needs four to five cycles. Due to the experimental device regulation, the climate cycles are defined with four temperature and relative humidity steps as shown on Fig. 3. The cycles given on the left are considered representative of cloudy days, north exposition and sunscreen effect. The cycles given on the right include the effect of solar radiation.

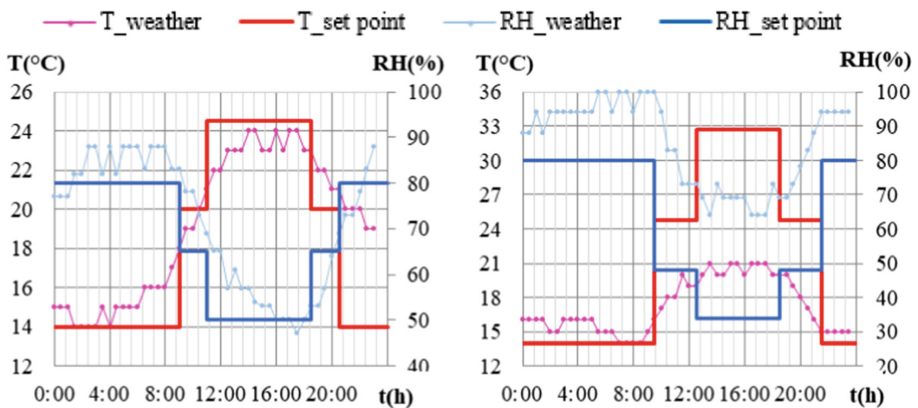


**Fig. 3.** Left: Ambient outdoor temperature and relative humidity without solar gains, Right: Equivalent temperature and relative humidity with solar gains for one typical day in Rennes in August

### 2.3 Results Analysis

For representative cycles, the kinetics of temperature, relative humidity and vapor pressure are given at each position and allow to plot profiles at several times along a day.

The results under dynamic solicitation are analyzed regarding dynamic parameters as the time lag and the relative amplitude variation, also called damping factor for the temperature (Fig. 4). The time lag is the time between the excitation at the outdoor surface and the response to the excitation. The relative amplitude variation is the ratio of the amplitude at the given point to the amplitude at the outdoor surface over the wall thickness.

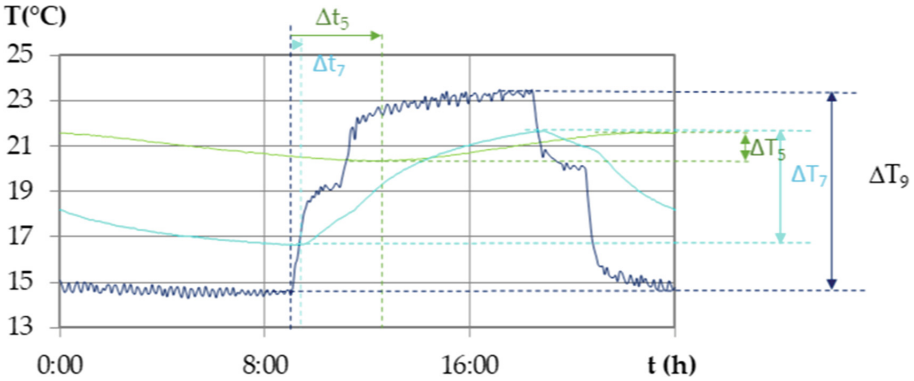


**Fig. 4.** Identification of the time lag  $\Delta t_i$  between the surface and a given point, and of the amplitude at the outdoor surface ( $\Delta T_9$ ) and at a given point ( $\Delta T_i$ ).

### 3 Results

#### 3.1 Impact on Temperature

Figure 4 displays the last cycle, it shows the indoor and outdoor ambient conditions are in good agreement with the set points. Over the repetition of cycles, the temperature beams increase, the wall heats up over its entire thickness in connection with the set points.

At night conditions, the outdoor temperatures are the same with or without solar radiation during the day. The heat flux induced by the temperature gradient goes from the inside to the outside. At daytime, without solar radiation, the indoor and outdoor temperatures are close and the heat flux is almost zero. Taking into account the solar radiation leads to equivalent outdoor temperature about 10 °C higher than those without solar radiation, and the heat flux goes from the outside to the inside (Fig. 5).

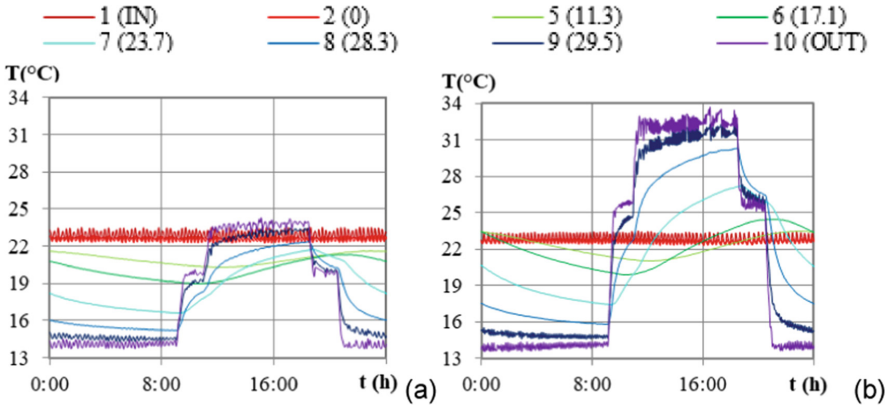


**Fig. 5.** Kinetics of temperature at several depth in the wall – a: without solar gains, b: with solar gains

The time lag and the temperature damping are similar for both cases, with or without taking into account the solar radiation. In fact, they depend only on the heat diffusion in the wall. The increase of the amplitude of the signal on the surface is translated by an increase of the amplitude of the signal in the thickness of the wall (Fig. 6).

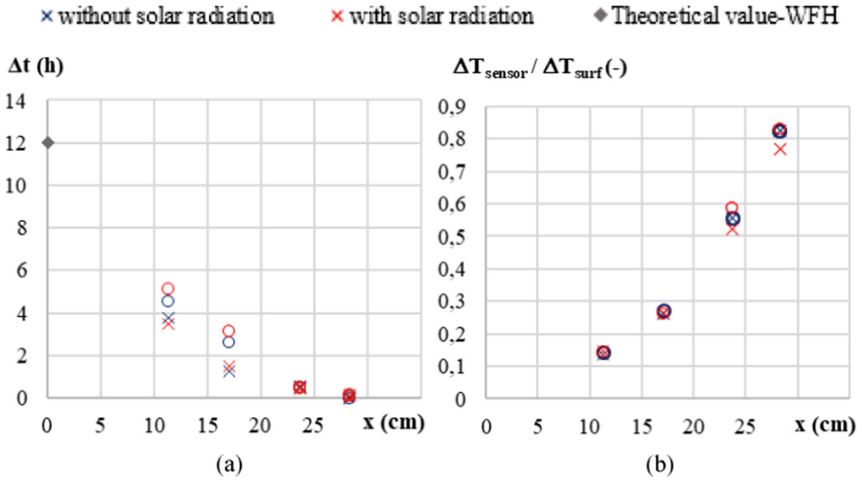


**Fig. 6.** Dynamic thermal parameters versus location ( $x$ /o: calculated during increasing/decreasing temperature step): (a) Shift of temperature (b) damping factor.

The temperature profiles are presented each hour during the last day of the dynamic study in Fig. 7. During the day, the temperature is almost constant on the inside surface of the wall, whereas on the outside surface, it evolves according to the set points.

Without solar radiation, the temperature profile shows a daily variation amplitude that evolves over the thickness of the wall. It is limited to the third of the thickness on the inner side and then increases towards the exterior. On the interior side, the temperature gradient is small to negligible but always negative. At the change of set point, the temperature increases on the outdoor surface. Then, in the core of the wall, the gradient of the temperature and the heat flow are reversed. The absorption of the heat flow on the outside leads to storage with a rapid increase in temperature in the outer layers.

With solar radiation, the increase of the temperature in the outside ambience during the day leads to an increase of the average temperature over the entire thickness of the wall. The increase of temperature on the outdoor surface leads to a propagation of heat that reaches the indoor side of the wall and induces a slight temperature gradient. This gradient of temperature reverses during the day and leads to slight delayed gains at night. This effect was not observed in the case where the sunlight was not taken into account. The two thirds of the wall thickness on the outdoor side are active and contribute to limit the heat gains on the indoor side.

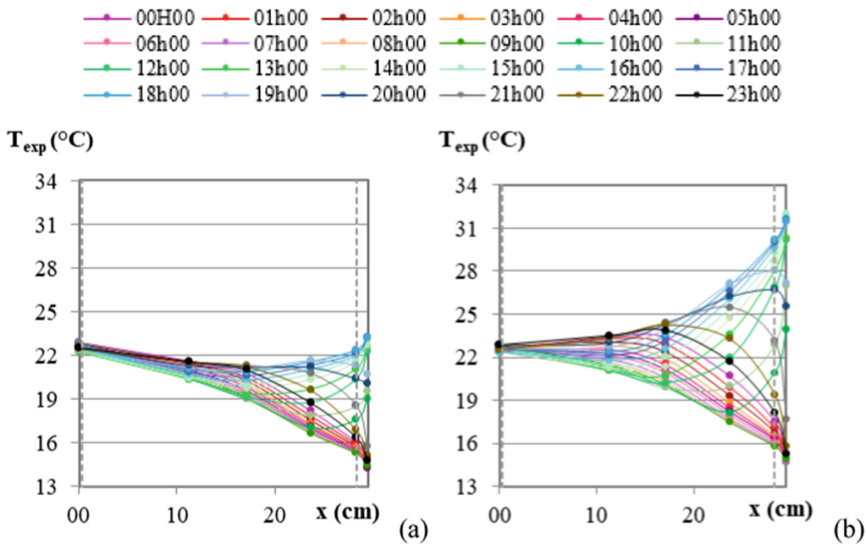


**Fig. 7.** Temperature profiles during the last day of the dynamic solicitation phase for the climate of Rennes; (a) without solar radiation, (b) with solar radiation

### 3.2 Impact on Vapor Pressure

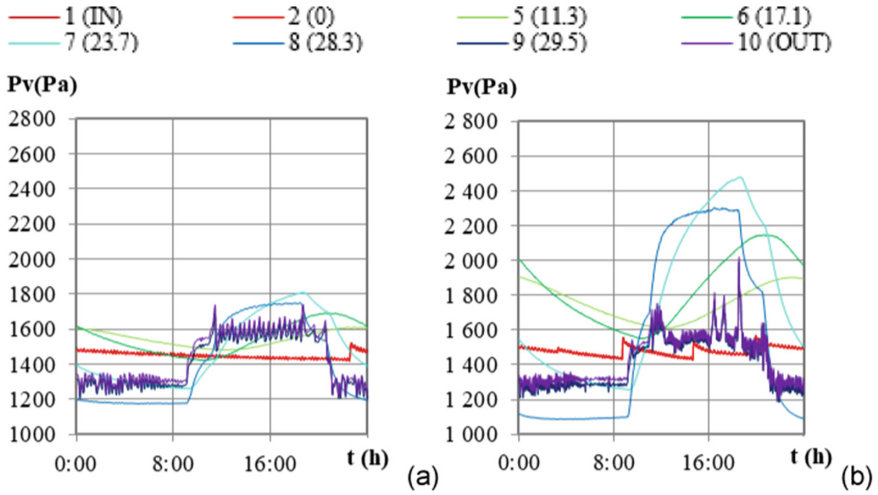
Figure 8 shows the vapor pressure kinetics at the different positions in the wall. For the vapor pressures, when considering solar radiation, the levels are higher than those observed during the solicitations without solar radiation, with higher amplitudes of variation. In addition, the vapor pressures within the wall are higher than those in the ambient conditions.

Figure 9 shows that the time lags are similar without and with solar radiation. The relative variations of the vapor pressure amplitude are higher when the effect of the solar radiation is considered. These values were higher than 1 on the external third in the case of solicitations without solar radiation and become higher than 1 on the whole thickness with solar radiation. This underlines the amplification of the desorption phenomena induced by the rise in temperature.

Figure 10 shows the vapor pressure profiles. During the daily cycle, the vapor pressure gradient reverses on the outdoor side of the wall, but not on the indoor side of the wall. When the effect of solar radiation is taken into account, the amplitude increases over the outdoor two-thirds of the wall. The maximum vapor pressure reached increases significantly due to the desorption phenomena related to the solar radiation. This leads to an increase of the vapor pressure all over the wall thickness, and a vapor pressure gradient on the indoor side about 2 times higher.

### 3.3 Impact on Heat Storage

Figure 11 shows the evolution of the heat fluxes on the indoor and outdoor surfaces of the wall under daily cyclic variations, without and with solar radiation. The experimental



**Fig. 8.** Kinetics of vapor pressure at several depth in the wall – a: without solar radiation, b: with solar radiation

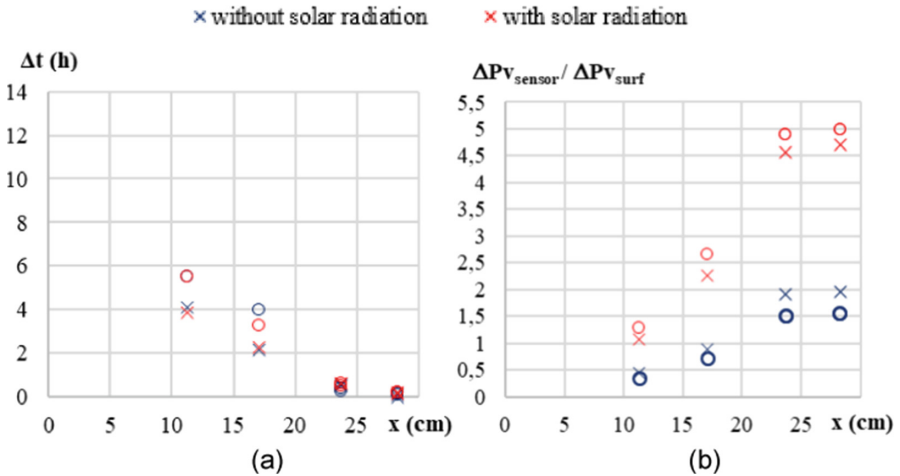


**Fig. 9.** Dynamic hygric parameters versus location ( $x/o$ : calculated during increasing/ decreasing vapor pressure step): (a) Shift of vapor pressure (b) damping factor

results show that the heat flux is repeated during the cycles in both cases. The change of the flux sign corresponds to the heat storage and release. The solar radiation enhances the heat exchanges on the outdoor surface. On the indoor surface, the heat flow remains very low because the heat flow does not reach this side of the wall, as seen on the profiles.

The integration of the fluxes on each surface gives the amount of heat stored and released by the wall. Figure 12 gives the total amount of heat stored and released over the last cycle. The effect of solar radiation leads to heat storage 3 times higher and heat release 1.2 times higher than without sun. The heat balance is nearly zero without solar



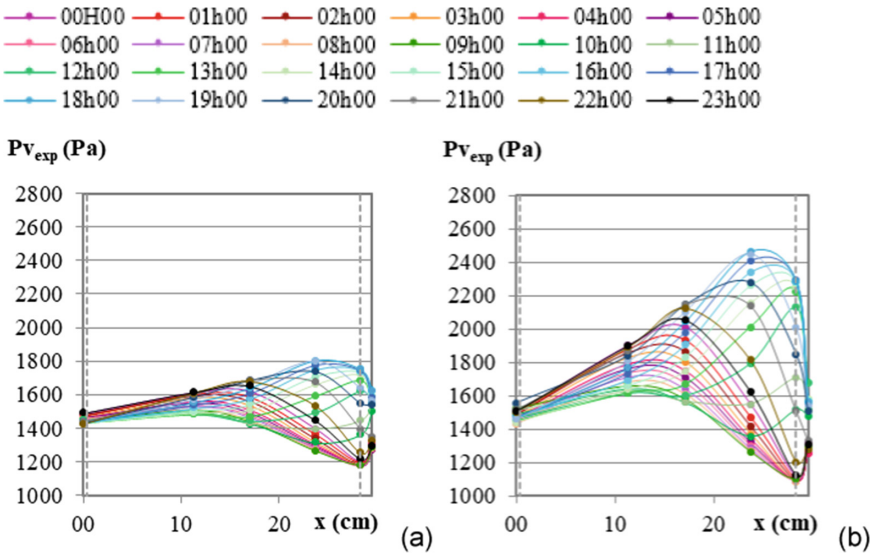


**Fig. 10.** Vapor pressure profiles during the last day of the dynamic solicitation phase for the climate of Rennes; (a) without solar radiation, (b) with solar radiation

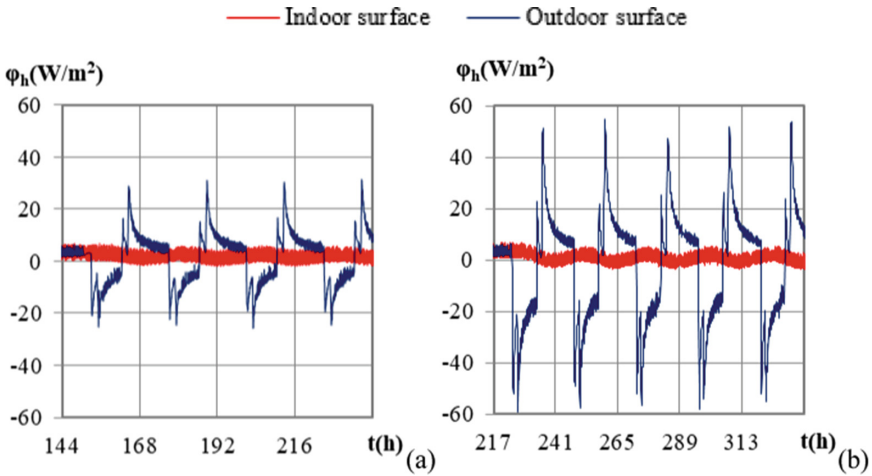


**Fig. 11.** Heat flux for the climate of Rennes; (a) without solar radiation, (b) with solar radiation

radiation and widely positive in the case with solar radiation, that induces an increase in the temperature of the wall.

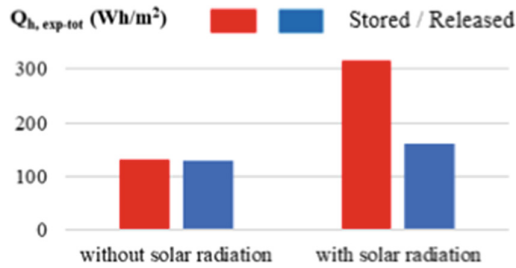


**Fig. 12.** Heat storage for the climate of Rennes without and with solar radiation

## 4 Conclusion

The investigation of the effect of the solar radiation on the hygrothermal behavior of a washing fines hemp wall highlights several key points.

With and without solar radiation effect, the main variations of temperature and vapor pressure occur over the two outdoor third of the thickness of the wall. Sorption-desorption phenomena are highlighted. Both temperature and vapor pressure variation and sorption-desorption phenomena are magnified with solar radiation.

## References

- Amziane, S., et al.: Bioaggregates based building materials, Springer Netherlands, Amziane Sofiane and Collet Florence (2017). <http://www.springer.com/la/book/9789402410303>. Accessed 24 February 24
- Boumediene, N., Collet, F., Pretot, S., Elouad, S.: Hygrothermal behavior of a washing fines—hemp wall under French and Tunisian summer climates: experimental and numerical approach. *Materials* **15**, 1103 (2022). <https://doi.org/10.3390/ma15031103>
- Collet, F., Prétot, S.: Experimental highlight of hygrothermal phenomena in hemp concrete wall. *Build. Environ.* **V82**, 459–466 (2014)
- Diagramme Solaire Interactif (2022). <http://diagsol.herokuapp.com/>
- Mazhoud, B., Collet, F., Pretot, S., Lanos, C.: Mechanical properties of hemp-clay and hemp stabilized clay composites. *Constr. Build. Mater.* **155** 1126–1137 (2017). <https://doi.org/10.1016/j.conbuildmat.2017.08.121>
- Mazhoud, B., Collet, F., Prétot, S., Lanos, C.: Effect of hemp content and clay stabilization on hygric and thermal properties of hemp-clay composites. *Construction and Building Materials* **300**(September), 123878 (2021). <https://doi.org/10.1016/j.conbuildmat.2021.123878>
- Medjelekh, D., Ulmet, L., Dubois, F.: Characterization of hygrothermal transfers in the unfired earth. *Energy Procedia.* **139**, 487–492 (2017). <https://doi.org/10.1016/j.egypro.2017.11.242>
- Météo France (2022). <https://meteofrance.com/>
- Seng, B., Magniont, C., Gallego, S., Lorente, S.: Behavior of a hemp-based concrete wall under dynamic thermal and hygric solicitations. *Energy Build.* **232** 110669 (2021). <https://doi.org/10.1016/j.enbuild.2020.110669>